



# Application of municipal solid waste (MSW) char during rotary drum co-composting (RDC) of vegetable waste and its characterization

Silvia Saikia<sup>1</sup> · Krishna Chaitanya Maturi<sup>2</sup> · Harsh Prit<sup>3</sup> · Suryateja Pottipati<sup>4</sup> · Ajay S. Kalamdhad<sup>3</sup>

Received: 14 March 2024 / Accepted: 4 July 2024

© The Author(s), under exclusive licence to Springer-Verlag GmbH Germany, part of Springer Nature 2024

## Abstract

Composting, a sustainable method for handling biodegradable waste constituting nearly 50% of municipal solid waste (MSW), can be enhanced by incorporating char produced from MSW pyrolysis. This study investigates the impact of MSW char (0% char—Control, 2.5% char—Trial 1, 5% char—Trial 2) on the physicochemical properties of vegetable waste compost. A thermophilic temperature range of 53.8 °C was detected in Trial 2, 50.8 °C in Trial 1, and 46.8 °C in Control. The pH of the mixes increased at day 20 to 7.5, 7.87, and 8.2 in Control, Trial 1, and Trial 2, respectively. The highest drop of total organic carbon (TOC) and volatile solids in Trial 2 is about 21.18% and 21.02%, respectively. Total Kjeldahl nitrogen (TKN) increased, particularly in Trial 2 (2.35%), while NH<sub>4</sub>-N concentrations decreased, and phosphorus levels rose notably to 23.48 mg/kg, with 2.49 mg/kg available phosphorus in Trial 2. The C/N was reduced to 10 in Trial 2. Total potassium increase was highest for Trial 1 (6.9 g/kg). Trial 2 had the highest overall macronutrient concentration and correspondingly showed the greatest decrease in volatile solids. Furthermore, Trial 1 demonstrated a reduction in heavy metal concentration in comparison to Control and Trial 2. Consequently, the utilization of MSW char during rotary drum composting enhances the process of composting and significantly improves compost quality, making it a sustainable waste management solution.

**Keywords** Char · Compost · Municipal solid waste · Pyrolysis · Rotary drum composting · Vegetable waste

---

Responsible Editor: Guilherme Luiz Dotto

## Highlights

The pH of the mixes increased at day 20 to 8.2 in the compost of 5% char (Trial 2).  
Thermophilic temperature range of 53.8 °C was detected in Trial 2.  
The C/N was reduced to 10 in Trial 2.  
In total, 2.5% char demonstrated a reduction in heavy metal concentration during composting.  
Trial 2 had the highest overall macronutrient concentration.

---

✉ Silvia Saikia  
ssilvia@iitg.ac.in

- <sup>1</sup> School of Agro and Rural Technology, Indian Institute of Technology Guwahati, Guwahati 781039, Assam, India
- <sup>2</sup> Department of Biology, Institute of Bioresource and Agriculture, Hong Kong Baptist University, Kowloon, Hong Kong
- <sup>3</sup> Department of Civil Engineering, Indian Institute of Technology Guwahati, Guwahati 781039, Assam, India
- <sup>4</sup> Department of Civil Engineering, National Institute of Technology Goa, Goa 403703, India

## Introduction

Over the past 20 years, significant research has been done on the advantages of utilizing biochar on land. The outcome of these studies has been reported as positive. The usage of compost in agronomy and its various aids to the quality of soil with time have been extensively clarified for several years (Guo et al. 2020). In the past 10 years, there has been a focus on utilizing a blend of biochar and compost as a final product for soil application. However, only a small fraction of these studies have focused on introducing biochar to the feed materials during composting and examining its subsequent effects on the process of composting the resulting co-composting product and its application in soil (Jain et al. 2018a, b). While the existing research predominantly indicates positive outcomes, there is a notable scarcity of studies concentrating on the enduring impacts of co-composting of biochar application (Gao et al. 2023). Consequently, it is strongly recommended that additional research be undertaken specifically aimed at assessing the potential of co-composting of biochar aging in agricultural soils. Biochar, when used as an additive in compost, enhances various

aspects of the composting process. It enhances composting efficiency, speeds up the process of humification, boosts microbial variety and activity, decreases the emission of greenhouse gases, and traps harmful metals in compost (Xiao-xia Guo et al. 2020). The presence of biochar during composting leads to a quicker rise in temperature and prolongs the thermophilic phase. Moreover, biochar improves the moisture retention capacity, thereby maintaining the optimal moisture level typically between 50 and 60% w/w in most composts when introduced at the onset of composting. It is important to acknowledge that biochars and composts originating from different sources exhibit diverse carbon-to-nitrogen (C/N) ratios that impact the rate at which organic matter decomposes (Godlewska et al. 2017). The biochar obtained through various processes like pyrolysis or hydrothermal carbonization and sourced from diverse materials displays a spectrum of pH levels, extending from alkaline to acidic. The leaching of alkaline and acidic compounds from biochar influences the pH of the surroundings, generating a conducive atmosphere for the activity of microbes (Murtaza et al. 2024). Moreover, certain types of biochar, characterized by high porosity and large specific surface area, serve as natural protective habitats that promote the proliferation of microbes. In specific biochar types, a high cation exchange capacity resulting from functional groups functions as an electron carrier, aiding in the transfer and transport of biochar (Antonangelo et al. 2021).

This heightened microbial activity plays a role in the mineralization of essential nutrients while concurrently reducing gas emissions (Jacoby et al. 2017). The integration of biochar into the composting procedure not only influences the compost itself and its functionality but also leads to significant modifications in biochar properties. For example, the cation exchange capacity of biochar rises post-composting, which is a beneficial trait for retaining nutrients and stabilizing pH levels (Munera-Echeverri et al. 2018). Co-composting of biochar, employed as a soil amendment, has demonstrated excellent efficacy in enhancing soil properties and promoting plant growth, as evidenced by studies (Awasthi et al. 2017; Oldfield et al. 2018; Wang et al. 2019). Its advantages also include alleviating soil drought (Lashari et al. 2013) and salinity pressures (Busch and Glaser, 2015), along with immobilizing organic pollutants and potential harmful metals (Ye et al. 2019; Teodoro et al. 2020). Furthermore, co-composting of biochar reduces the bioavailability of these substances to plants and soil microorganisms (Rodríguez-Vila et al. 2016). The favorable results allied to co-composting with biochar exceed those when simply blending the biochar with the final compost product, potentially owing to interactions between the two components throughout the process of composting.

The objective of the study is to present current findings regarding the impact of MSW char addition on the

composting process. Also, a detailed analysis was done to explore the resulting product from the co-composting of MSW char and vegetable waste in a rotary drum composting and to assess its application in agriculture and soil contaminated with metal. Additionally, this manuscript provides a concise overview of the most recent research on using co-composed char products to enhance the quality of soil, increase plant yields, and mitigate the bioavailability of potentially toxic metals to crops and animals. The primary aim is to enhance the production of co-composting of char and application in agriculture, serving as a foundation for future research endeavors. The presented overwhelming evidence demonstrates the numerous advantages that outweigh the drawbacks of employing co-composted MSW char to enhance the fertility of soil and plant yield while also highlighting the viability of utilizing this product for remediating soils contaminated with potentially toxic metals.

## Materials and methods

### Sample collection and preparation

The MSW sample was collected from the Boragaon dumpsite, the sole disposal site in Guwahati, which is located in northeastern India. After conducting a compositional analysis, the combustible portion of the waste was selected as pyrolysis feedstock, which consists of paper, plastic, rubber, leather, cardboard, clothes, and biomass material such as coconut shells and husk, wood, tree branches, and leaves (see supplementary material). For co-composting, vegetable wastes were collected from the different hostel messes of the Indian Institute of Technology Guwahati (IITG), and fresh cow dung was used as an inoculum to enhance the microbial activity in the study. The moisture content of vegetable waste and cow dung was very high (Table 2), so to avoid the probability of generation of leachate, a bulking agent such as grass cutting, dry leaves (collected from the vicinities of IITG), and sawdust (collected from a sawmill located in Amingaon, Guwahati, Assam) was mixed during the composting process as shown in Figs. 1 and 2 (Sudharsan Varma and Kalamdhad 2015).

### Pyrolysis of MSW for char production

In each batch of pyrolysis experiment, 2 kg of combustible fragment of MSW, without segregation or shredding, was placed on the grate inside the pyrolyzer, as depicted in Fig. 1. To preserve an inert atmosphere within the reactor, nitrogen gas was introduced through an inlet valve, while the pyrolysis gas produced was condensed in ice bath. Subsequently, the

reactor was equipped with a temperature controller and operated at 250 °C, with a heating rate of 10 °C/min, and a holding time of 180 min, as per the optimized conditions for achieving the highest yield of MSW char in a fixed bed pyrolyzer (Saikia and Kalamdhad 2023). The MSW char formed was collected from the grate and used for further analysis.

### Co-composting of MSW char and vegetable waste

Co-composting was done utilizing in-vessel composting in the rotary drum composter (RDC), which outperforms all other composting methods in terms of degradation rate and waste materials stabilization (Singh and Kalamdhad 2016; Sharma et al., 2017). Therefore, a retention period of 20 days was selected for the experiment. The lab-scale RDC had a volume capacity of 550 l and operated in batch mode, as shown in Fig. 3. The apparatus is affixed to a metal frame with four rubber rollers and is mechanically rotated using a handle. The main body of the drum was made from mild steel and has dimensions of 1.022 m in length and 0.76 m in diameter. Inside the drum, 40×40 mm angles are welded along its length to facilitate proper blending, stirring, and aeration of feedstock during rotation (Maturi et al., 2022b). Additionally, two head-to-head holes, each 10 cm in diameter, are positioned at the top to allow for the drainage of additional water. Rotation of the RDC was done manually every 24 h to ensure appropriate aeration. Three different composting ratios of vegetable waste, sawdust, cow dung, and MSW char were added in three different rotary drum composters comprising 100 kg of waste materials. Vegetable wastes were cut into 2 to 5 cm in size by the mechanical shredder for the uniform blending of the composting material. The optimal blend consisting of cow dung, vegetable waste, and sawdust was prepared, taking into account their respective mixing ratios as documented in previous studies on the RDC of vegetable waste (Sudharsan Varma and Kalamdhad 2015). The addition of more than 20% of the MSW char is not recommended as it may interfere with the biodegradation of organic waste (Camps and Tomlinson 2015). As shown in Table 1, 2.5% and 5% (w/w) MSW char was added to the 100 kg of waste material, and it was homogenized and mixed before it was put in the rotary drum.

### Sampling

Sampling was conducted on even alternative days throughout the 20 days. From each reactor, triplicate samples were collected at three specific locations, each 20 cm from the surface and distinct from one another. A portion of the samples was kept at 4 °C for immediate biological examination, while some were air-dried, crushed, and sieved for subsequent physicochemical analysis.

### Physicochemical and nutritional parameters

The temperature was monitored every 6 h with the help of a digital thermometer. To measure pH and electrical conductivity, approximately 10 g of the compost sample, which was sieved through a 0.22-mm sieve, was mixed with 100 mL of distilled water in a 1:10 ratio (w/v). The mixture was then subjected to horizontal shaking for 2 h at 120 rpm. Subsequently, the pH of the suspension was determined using the pH meter. The conductivity of the suspension was measured using the EC meter. To measure volatile solids, approximately 10 g of the compost was placed in a crucible ( $W_1$ ), which was subsequently placed in a muffle furnace for 2 h at 550 °C. After this duration, the final weight of the sample was recorded as  $W_2$ . The measurement of volatile solids in the sample was calculated as follows according to the Brandi (2013) standard method:

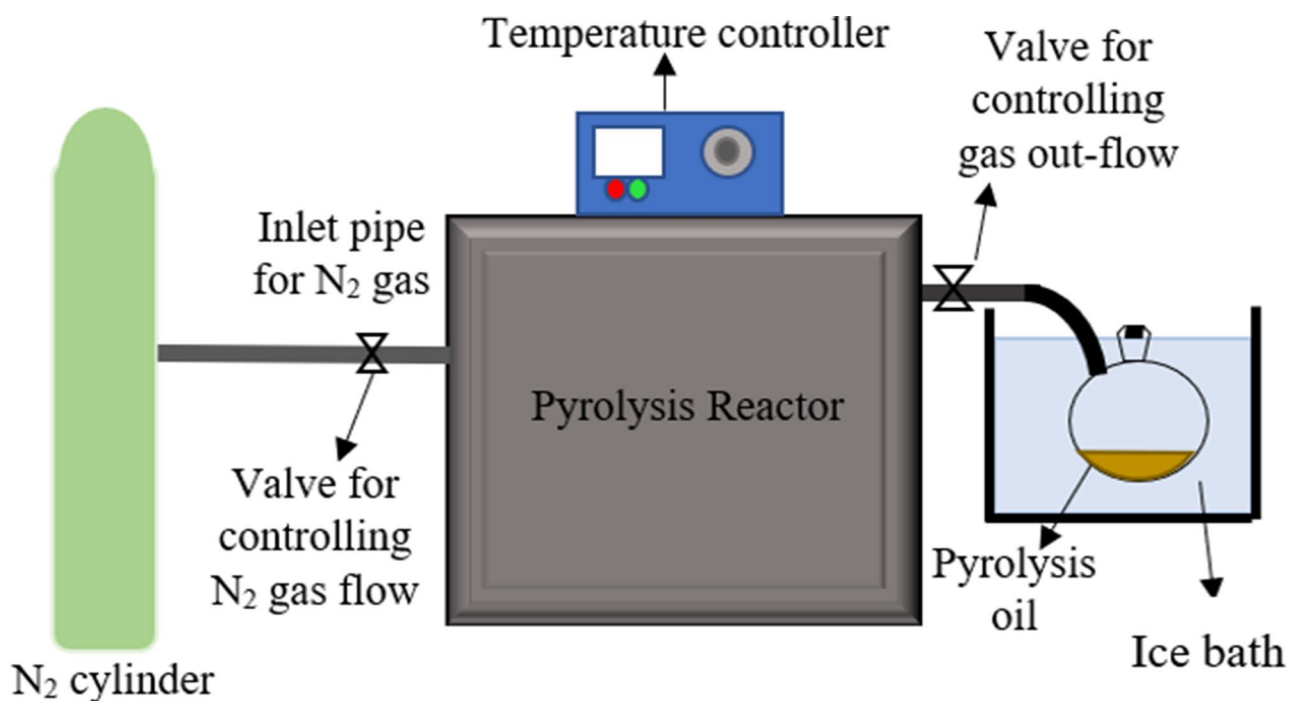
$$VS = \frac{(10 - (W_2 - W_1))}{10} \times 100 \quad (1)$$

Total organic carbon was determined by dividing the value of the volatile solids by factor 1.8, according to the Brandi (2013) standard method (Maturi et al. 2022a). The ash content was determined according to Maturi et al. 2022a. TKN was measured using the Kjeldahl distillation method. For this procedure, approximately 0.2 g of dried sample was mixed with a catalyst mixture consisting of 3 g of potassium sulfate and cupric sulfate in a 5:1 ratio. The mixture was then digested with 10 mL of  $H_2SO_4$  at 400 °C for a duration of 4 h. After digestion, the volume of the digested sample was diluted to 100 mL and underwent distillation using the Kelplus distillation unit (Kausar et al. 2020). The distilled samples were titrated using 0.02 N  $H_2SO_4$ /0.01 N  $H_2SO_4$ .

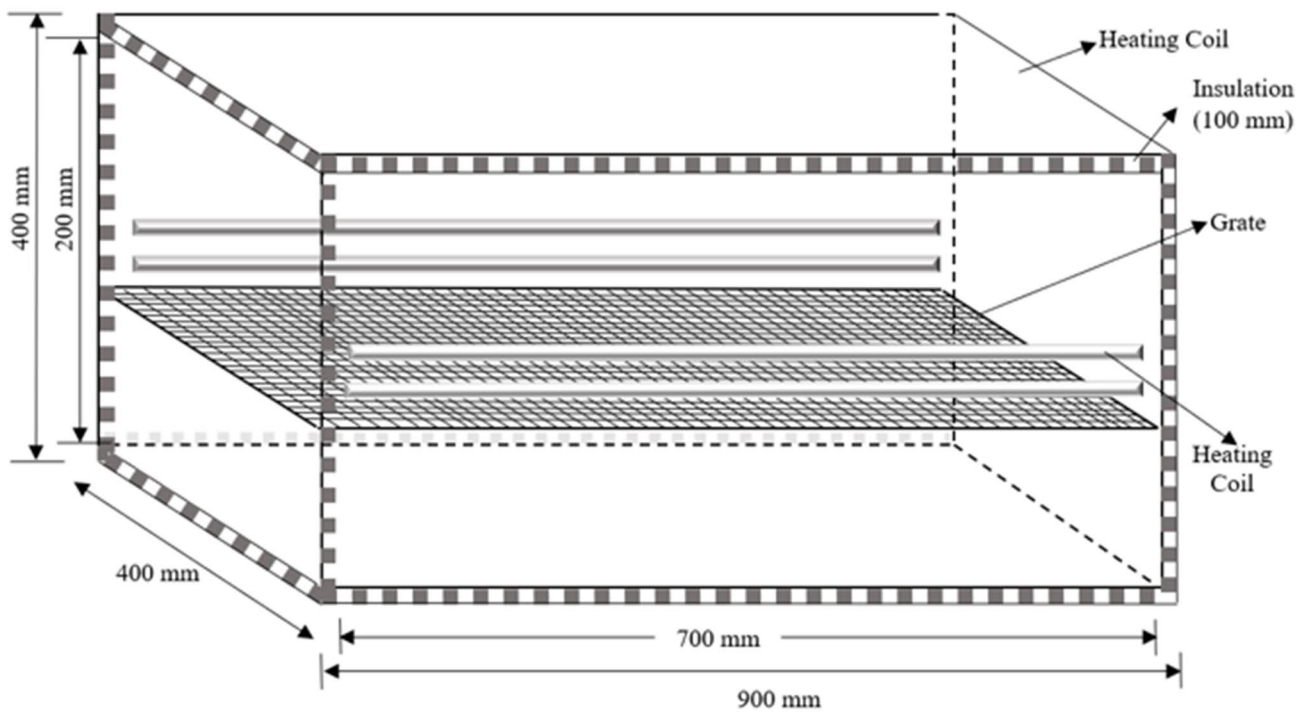
$$TKN = \frac{14 \times (S - B) \times N}{\text{Weight of the sample}} \quad (2)$$

In this context,  $S$  represents the volume of standard sulfuric acid used for the sample,  $B$  represents the volume of standard sulfuric acid used for the blank,  $N$  signifies the normality of the standard sulfuric acid, and  $W$  denotes the weight of the compost sample in grams.

The nitrate ( $NO_3$ -N) and ammonical nitrogen ( $NH_4$ -N) were determined spectrophotometrically after extraction with a 2 M KCL solution (Varma et al. 2018). Determination of available phosphorus and total phosphorus is done by colorimetric method according to the Brandi (2013) standard method (Kausar et al. 2020). The overall concentration of sodium, potassium, and calcium was assessed using a flame photometer (Systronic 128) after digestion of the 0.2 g sample in a block digester with 10 mL of mixed acid ( $H_2SO_4$  and  $HClO_4$  in ratio 5:1) (Kausar et al. 2020).



(a)



(b)

**Fig. 1** **a** Pyrolysis setup using fixed bed reactor and **b** internal perspective of pyrolysis reactor

## Heavy metal analysis

Total concentrations of heavy metals such as iron (Fe), lead (Pb), manganese (Mn), zinc (Zn), chromium (Cr), copper (Cu), and nickel (Ni) were determined by atomic adsorption spectrometer (AAS) (Varian Spectra 55B).

## Biological analysis

### Evolution of CO<sub>2</sub>

According to Kalamdhad et al., (2008), the direct approach to assess the stability of compost is CO<sub>2</sub> evolutions measured by static measurement method. About 10 g of soda lime was oven-dried and mixed with 25 g of fresh compost inside a container. The evolution of CO<sub>2</sub> was calculated as follows (Kalamdhad et al. 2008):

$$\text{CO}_2 \text{ evolution (mg/gVS/day)} = \frac{W_2 - W_1}{W \times T} \times 1000 \quad (3)$$

In Eq. (3),  $W_1$  and  $W_2$  represent the initial and final weight of the soda lime (in grams) after incubated at 25 °C and oven-dried, respectively,  $W$  denotes the weight of the compost sample (in grams), and  $T$  indicates the period of incubation (in hours).

### Soluble biochemical oxygen demand (sBOD) (APHA, 2005)

The sample was diluted in a ratio of 1:10 and placed on a horizontal shaker for 2 h. Following this, the solution was filtered, and the resulting supernatant was collected for analysis of BOD using the BOD5 test.

$$\text{sBOD} = \frac{D_1 - D_2}{P} \times \text{DF} \quad (4)$$

In this context,  $D_1$  and  $D_2$  represent the initial and final levels of dissolved oxygen in the sample after 5 days of incubation, measured in mg/L,  $P$  denotes the volume of the sample diluted to a total volume of 300 mL with dilution water, and DF equals dilution factor.

### Soluble chemical oxygen demand (sCOD) (APHA, 2005)

The sCOD analysis was conducted by diluting the compost in a 1:10 ratio, and the resulting filtrate was analyzed using the closed reflux method. In this method, 1.5 mL of K<sub>2</sub>Cr<sub>2</sub>O<sub>7</sub>

and 3.5 mL of H<sub>2</sub>SO<sub>4</sub> reagent were mixed with 2.5 mL of the filtered sample in a COD vial. The mixture was then digested for 2 h at 150 °C and subsequently cooled to ambient temperature. It was then titrated against ferrous ammonium sulfate (FeH<sub>8</sub>N<sub>2</sub>O<sub>8</sub>S<sub>2</sub>) using a ferroin indicator until the color changed from green to deep red hue (Kausar et al. 2020)

$$\text{sCOD} = \frac{(A - B) \times M \times 8000}{\text{ml of sample}} \quad (5)$$

In this scenario,  $A$  and  $B$  represent the volume of FeH<sub>8</sub>N<sub>2</sub>O<sub>8</sub>S<sub>2</sub> used for the blank and sample, respectively;  $M$  denotes the molarity of FeH<sub>8</sub>N<sub>2</sub>O<sub>8</sub>S<sub>2</sub>, and 8000 signifies the milliequivalent weight of oxygen multiplied by 1000 mL/L.

## Microbial analysis

Ten grams of fresh samples were placed into 100 mL of sterile distilled water in an Erlenmeyer flask. The solution is mechanically mixed at 220 rpm in a horizontal shaker. The diluted samples were inoculated in culture media tubes to measure the amount of total and Fecal coliform using the most probable number (MPN) (APHA 2012). Total counts of heterotrophic bacteria were determined by inoculation of diluted samples in culture media Petri dish using the pour plate method (APHA, 2015).

## Results and discussions

### Initial characterization of substrate

The preliminary characterization of the composting material char is shown in Table 2. The moisture content of vegetables was very high (89.23%), whereas the moisture content of MSW char was very low, about 1.14%. To avoid leachate formation during the composting process and to optimize the C/N ratio, bulking agent sawdust was used. The presence of optimum moisture is significant for regulating temperature within the compost pile. Composting is characterized as an exothermic phenomenon, signifying its capacity to produce thermal energy. The presence of appropriate moisture levels promotes the effective dispersion of heat inside the pile, hence sustaining the optimal temperature range required for decomposition. The initial pH values of vegetable waste, cow dung, sawdust, and MSW char were 5.87, 6.2, 6.35, and 7.10, respectively. These values fell within the optimal range for fungal growth (5.0–8.5) and bacterial development (6.0–7.5) (Meena et al. 2021). The electrical conductivity of vegetable waste measured at 1.93 mS/cm indicates a low

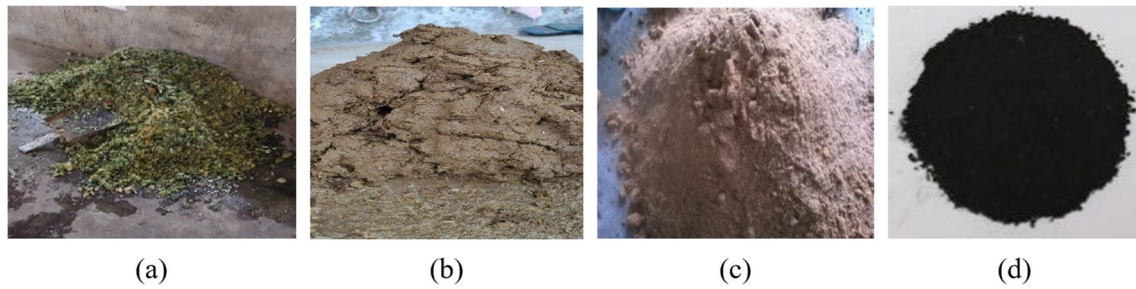


Fig. 2 a Vegetable waste, b cow dung, c sawdust, d MSW char

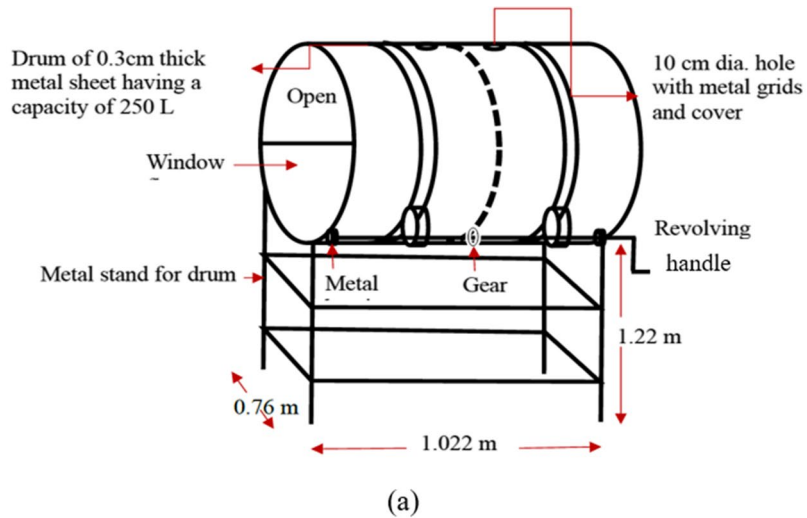


Fig. 3 Schematic diagram of rotary drum composter and b and c rotary drum composter

Table 1 Mix proportion of composting material and MSW char

Trial name	Mixed proportions	Vegetable waste (kg)	Cow dung (kg)	Saw dust (kg)	Total (kg)	MSW char (%) added
Control	5:4:1	50	40	10	100	0
Trial 1	5:4:1	50	40	10	100	2.5
Trial 2	5:4:1	50	40	10	100	5

presence of soluble salts, reflecting the material salinity arising from exchangeable chloride, sodium, sulfate, nitrate, potassium, and soluble salts or due to the presence of highly conductivity metal ions (Feng et al. 2021). The sBOD of vegetable waste was higher than cow dung, indicating more degradable carbonaceous materials (Mangkoedihardjo et al., 2006). Vegetable waste also contained 79.84% volatile solids, 2.45% TKN, and 18.51 g/kg of total phosphorus, which resembles nutrient richness and is a feasible option for composting (Maturi and Kalamdhad 2024). The C/N ratio of sawdust indicated a higher amount of carbonaceous matter. The fecal coliform of cow dung was  $2.4 \times 10^{11}$ , which determines the high concentrations of pathogenic bacteria (Hazarika and Khwairakpam 2018). The concentration of Ca, K, Mg, and Na was in the order of  $Ca > K > Mg > Na$  for Control, Trial 1, and Trial 2. The initial concentration of metals in MSW char was observed to be high, as depicted in Table 2.

## Variation of temperature and moisture content during the composting process

The vegetable waste, which contains the highest quantity of organic content, triggers the activity of microbes at the onset of the composting process, resulting in a rise in temperature. This temperature increase was observed during the initial phases of composting, i.e., within 12 h in Control, Trial 1, and Trial 2. The highest temperature of 53.8 °C was observed when 5% MSW char was applied in Trial 2, followed by 50.8 °C in Trial 1 and 46.8 °C in Control, as shown in Fig. 4a. The thermophilic phase lasted longer in Trial 2 due to the cumulative increase of MSW char, which was comparable to biochar amendment during composting (Jain et al. 2018a, b). The rise in temperature during the composting process is attributed to the destruction of pathogenic bacteria and a higher rate of decomposition of biodegradable carbon. The introduction of MSW char elevates

**Table 2** Initial characterization of substrate

Parameters	Vegetable waste	Cow dung	Saw dust	MSW char
Moisture content %	89.23 ± 0.23	90.08 ± 1.24	13.2 ± 0.2	1.14 ± 0.13
pH (1:10)	5.87 ± 0.09	6.2 ± 0.12	6.35 ± 0.14	7.10 ± 0.04
EC (1:10)	1.93 ± 0.08	2.93 ± 0.11	1.29 ± 0.08	3.57 ± 0.15
Oxygen uptake rate	30.4 ± 0.7	21.9 ± 0.61	8.90 ± 0.9	-
CO <sub>2</sub> evolution rate	21 ± 1.12	13 ± 1.30	9 ± 1.23	-
Volatile matter %	79.84 ± 1.23	84.8 ± 2.78	91.27 ± 1.25	21.13 ± 0.31
Ash content %	20.16 ± 1.11	15.2 ± 2.33	8.73 ± 0.98	2.83 ± 0.36
TOC %	44.36 ± 1.23	47.11 ± 2.79	50.71 ± 1.21	1.83 ± 0.67
TKN %	2.45 ± 0.14	0.84 ± 0.14	0.28 ± 0.07	0.42 ± 0.02
C/N ratio	18.1 ± 0.45	56.1 ± 0.23	181.1 ± 3.87	5.07 ± 0.03
Ammonia (mg/kg)	106.26 ± 0.41	179.4 ± 1.5	88.93 ± 0.11	18.91 ± 0.23
Nitrate (mg/kg)	20.54 ± 0.12	2.46 ± 0.19	17.07 ± 0.67	61.78 ± 0.13
sCOD (mg/L)	2880 ± 17	1152 ± 23	768 ± 12	-
sBOD (mg/L)	1020 ± 19	645 ± 14	195 ± 19	-
Total phosphorus (g/kg)	18.51 ± 0.32	12.25 ± 0.4	2.5 ± 0.2	7.23 ± 0.29
Available phosphorus (g/kg)	1.04 ± 0.23	2.45 ± 1.01	0.87 ± 0.42	3.14 ± 0.13
Fecal coliform	-	$2.4 \times 10^{11}$	-	-
Mg (g/kg)	2.75 ± 0.65	3.12 ± 0.4	1.28 ± 0.3	4.25 ± 0.28
K (g/kg)	5.23 ± 0.8	0.16 ± 0.12	0.8 ± 0.14	9.18 ± 0.3
Ca (g/kg)	39.39 ± 2.21	39.23 ± 3.40	21.9 ± 1.76	7.46 ± 0.12
Na (g/kg)	3.72 ± 0.8	3.23 ± 0.7	1.67 ± 0.9	3.05 ± 0.3
Mn (mg/kg)	996.15 ± 3.2	521.55 ± 4.5	483.55 ± 2.1	204.12 ± 0.5
Fe (mg/kg)	10,229 ± 7.67	9547.75 ± 8.98	6439.4 ± 7.43	2234.81 ± 61
Cr (mg/kg)	78.3 ± 0.97	142.8 ± 0.87	40.8 ± 0.78	83.42 ± 2.65
Pb (mg/kg)	996.5 ± 1.23	525 ± 3.12	483.55 ± 5.23	345 ± 2.12
Cd (mg/kg)	< BDL	< BDL	< BDL	< BDL
Cu (mg/kg)	101.8 ± 1.67	57.5 ± 2.12	205.1 ± 2.34	117.63 ± 0.12
Ni (mg/kg)	365.1 ± 4.23	320.9 ± 6.12	244.25 ± 2.89	213.45 ± 1.45
Zn (mg/kg)	213 ± 2.10	156.7 ± 7.55	143.54 ± 5.97	419.24 ± 4.12

The data is presented in  $xx \pm yy$  format where  $xx$  denotes the average value  $yy$  denotes the standard deviation, BDL: below detection level

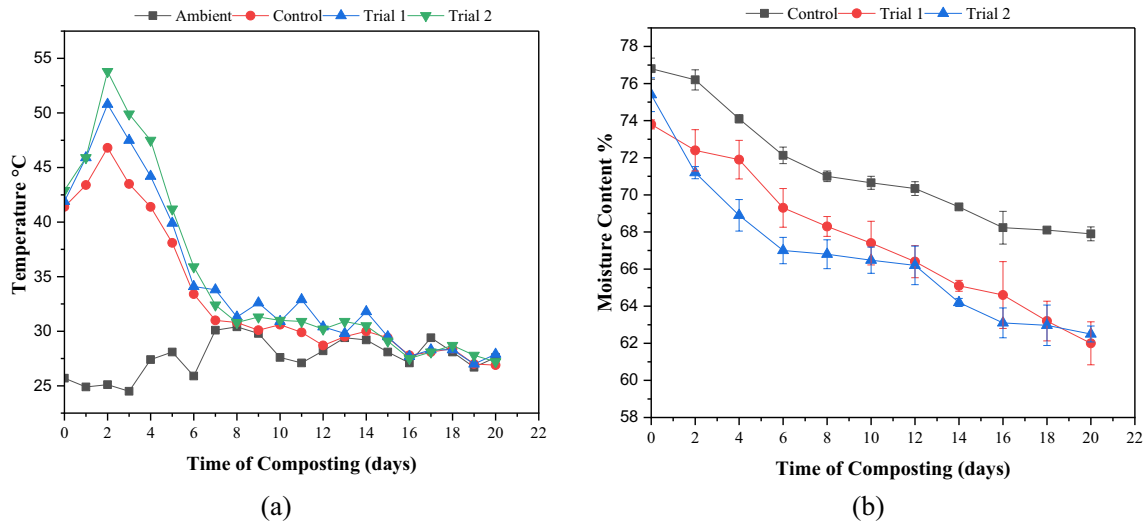


**Fig. 4** Changes in **a** temperature and **b** moisture content during the process of composting

the maximum temperature and accelerates the timeframe to attain high temperatures. This is attributed to the increased porosity caused by the addition of MSW char during the composting, facilitating greater oxygen availability. Consequently, the heightened porosity boosts the metabolic activities of microorganisms, leading to increased heat release. Additionally, the incorporation of char extends the duration of the high-temperature phase, as MSW char effectively sustains elevated temperatures owing to its microporous structure. However, excessive MSW char can elevate temperatures excessively, leading to undesirable moisture loss, which is unfavorable for composting (Jain et al. 2018a, b).

The moisture content of vegetable waste (89%) and cow dung (90%) was very high. To avoid leachate formation due to organic waste with high moisture content and for proper circumferential degradation, bulking agents such as grass cutting, dry leaves, sawdust, and MSW char were minced with inoculum and the substrate. Maturi et al., (2022a) reported that microbial activity decreases at low moisture content, and at high moisture content, the composting process slows down to anaerobic conditions. The rise in temperature was observed in a few days due to readily biodegradable matter, and there was no formation of leachate during the process of composting. The heat produced due to biological decomposition results in vaporization or moisture loss due to the rise in the rate of the decomposition process (Jain et al. 2018a, b). The inclusion of MSW char led to a decrease in moisture content, as depicted in Fig. 4b. This occurred as the addition of char lowered bulk density, promoting improved aeration and enhanced microbial activity. Consequently, there was increased heat loss, leading to greater moisture evaporation comparable to the moisture loss with biochar application during composting (Jain et al. 2018a, b). Additionally, char contributed to the loosening of

the compost structure, facilitating enhanced ventilation. This, in turn, boosted microbial activity, resulting in increased water absorption by the microbes.

### Variation of pH and electrical conductivity

The pH has a significant impact on microbial activity, and it has been observed that a neutral pH is optimal for the composting process. Metabolic process is more at 7.5–8.5 (Wong et al. 2009). The initial pH of mixes was recorded as 6.6, 6.72, and 6.84, which was increased to 7.5, 7.87, and 8.2 in Control, Trial 1, and Trial 2, respectively, as shown in Fig. 5a. The introduction of MSW char in the process of composting elevates the pH values in all treatments during the initial warming stage compared to the control. The pH of the final compost with the addition of MSW char was within the range of the pH of the biochar-added compost (7.4–8.5) (Jain et al. 2018a, b). In the warming phase,  $\text{NH}_3$  is generated, facilitating the breakdown of organic matter by bacteria and fungi. Subsequently, the pH gradually decreases in the middle and concluding stages of composting as bacteria and fungi convert some organic matter into organic acids, aiding the breakdown of lignocellulosic structures. During the cooling period, the pH stabilizes. Additionally, the ash content of char, containing  $\text{Na}^+$ ,  $\text{Ca}^+$ ,  $\text{K}^+$ , and  $\text{Mg}^+$ , undergoes ion exchange with  $\text{H}^+$  ions, further contributing to an increase in pH.

The EC value higher than  $4 \text{ mScm}^{-1}$  causes a toxic effect on plants after its application (Qu et al. 2022). At the beginning of the composting process, the EC value was maximum, resulting from the release of ammonium ions and salts due to increased biodegradation of organic matter during the thermophilic phase. As shown in Fig. 5b, with the application



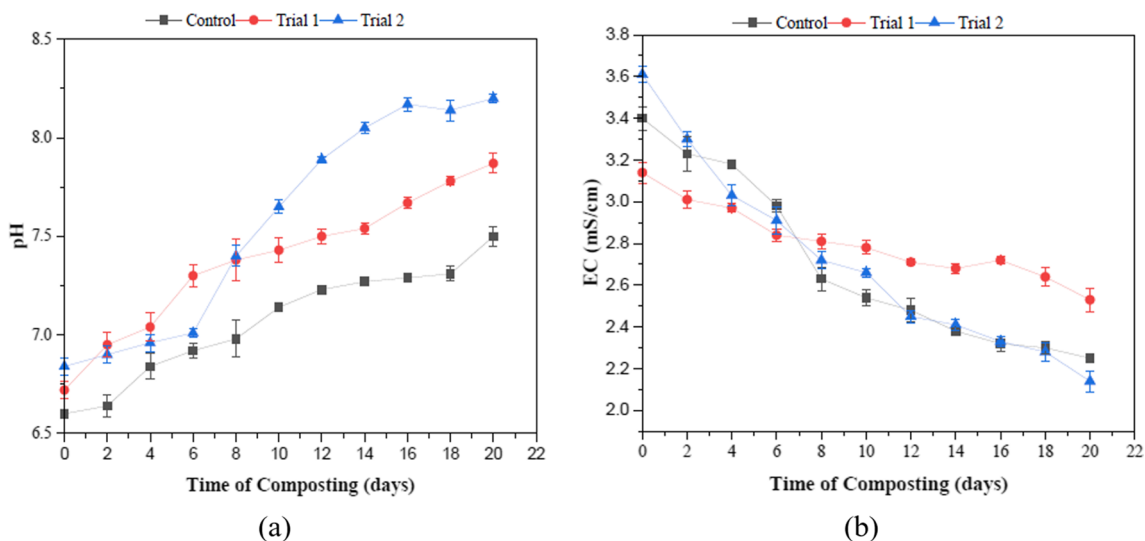


**Fig. 5** Variation of **a** pH and **b** electrical conductivity

of MSW char in Trial 1, it was detected that the EC values reduced in the later stage of composting as compared to control due to precipitation of mineral salts, volatilization of ammonia, and conversion of  $\text{NH}_4^+$  into nitrate. Moreover, humification might bind small molecules during the maturation phase, lowering their abundance in the solutions obtained from solid samples through water extraction for EC analysis (Feng et al. 2021).

### Variation of volatile solid, total organic carbon, and ash content during the composting period

The greater the volatile solids concentration, the higher the content of organic matter. When MSW char was introduced, Trial 2 exhibited a maximum reduction of 21.02% in volatile solids, in contrast to 19.11% in Trial 1 and 17.67% in the Control, as shown in Fig. 6a. Maximum reduction of volatile solids was observed in the thermophilic phase as thermophilic bacteria decompose the organic matter rapidly (Jain et al. 2018a, b). Initially, TOC was in the range of 27.28, 33.26, and 26.82%; after the application of MSW char, it finally reduced to 22.35, 26.17 and 21.18% in Control, Trial 1, and Trial 2, respectively, during the co-composting process, as depicted in Fig. 6b. Consumption of organic carbon as an energy source by microbes and  $\text{CO}_2$  produced by bacteria during the metabolic process are causes of the decrease of TOC during the process of composting (Daga et al., 2018). As shown in Fig. 6c, the ash content increases by 14.82, 26.65, and 19.62% in Control, Trial 1, and Trial 2, respectively, due to organic matter degradation and high ash content of MSW char. The decrease in volatile solids synchronized with an increase in ash content in all three treatments.

### Nitrogen dynamics (TKN and $\text{NH}_4\text{-N}$ ) and phosphorus (total phosphorus and available phosphorus) dynamics during the composting period

Nitrogen and phosphorus are the essential macronutrients that are required by the plant for its growth. The TKN was observed in the range of 0.96, 1.12 and 1.19% on day 0 and increased to 2.17, 2.24, and 2.35% on day 20 in Control, Trial 1, and Trial 2, respectively, as shown in Fig. 7, which was in the range of increase in the percentage of TKN value with the amendment of biochar during composting (Jain et al. 2018a, b). Because of the overall loss of dry mass caused by  $\text{CO}_2$  emission and water loss due to evaporation resulting from the heat generated during the oxidation of organic material, TKN increased during the rotary drum composting process. In the cooling phase, there is a gradual rise in TKN content. The inclusion of MSW char facilitates the breakdown of cellulose, supplying nutrients to the composting process. Additionally, char contributes to nitrogen fixation, serving as a source of nitrogen for the growth and reproduction of microorganisms (Qu et al. 2022). The  $\text{NH}_4$  was observed in the range 94.12, 102.49, and 93.41 mg/kg on day 0, reducing to 34.1, 38, and 32.37 mg/kg on day 20 in Control, Trial 1, and Trial 2, respectively, which was comparable to the biochar application during composting of various substrate (Xiao xia Guo et al. 2020). The result shows that the concentration of  $\text{NH}_4\text{-N}$  has significantly decreased throughout all treatments, and the decrease was greater when 2.5% MSW char was added in Trial 1. As the temperature increases rapidly with the addition of MSW char, the composting enters the high-temperature phase where volatilization of  $\text{NH}_3$  takes place, which results

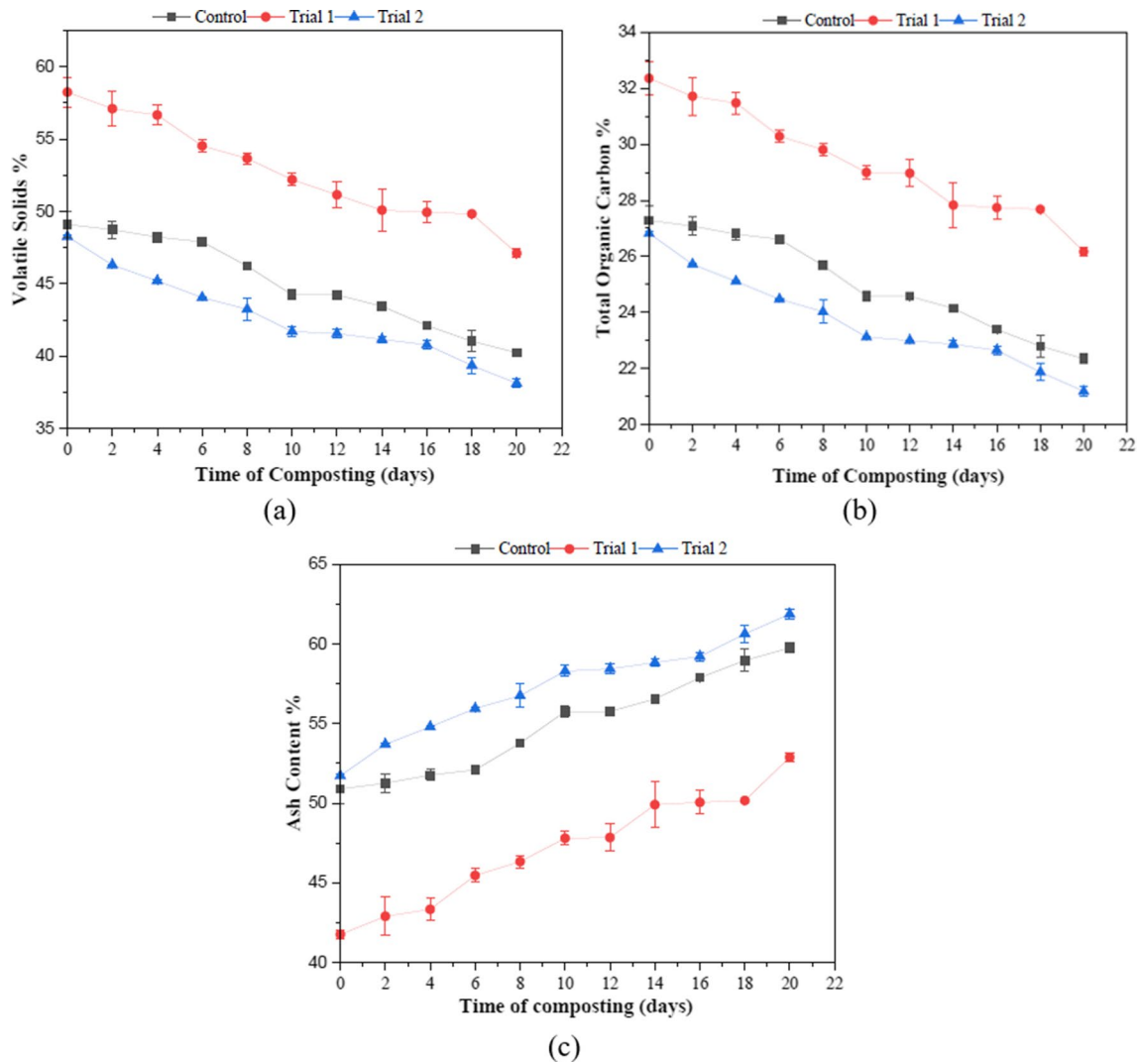


**Fig. 6** Variation of **a** volatile solid, **b** total organic carbon, and **c** ash content during the process of composting

in a decrease of the  $\text{NH}_4^+\text{-N}$  content, which is similar to the case of biochar amendment (Agyarko-Mintah et al. 2017). The organic nitrogen transforms to ammoniacal nitrogen in the initial period of the composting process. Due to intense aeration, a significant rise in pH, and the loss of  $\text{CO}_2$  during the process,  $\text{NH}_4^+\text{-N}$  decreases during the maturation stage (Kausar et al. 2020). The high amount of total phosphorus was observed on the initial day, which may have been caused by a higher concentration of vegetable waste, cow dung, and MSW char (Kalamdhad et al. 2008). During the process of composting, total phosphorus increased from 14.13, 14.1, and 16.79 mg/kg to 20.1, 20.89, and 23.48 mg/kg in Control, Trial 1, and Trial 2, respectively. The percentage increase of total phosphorus was highest about 6.7%, when 5% of MSW char was applied. Available phosphorus increased from 0.84, 0.95 and 1.02 mg/kg to 2.28, 2.38, and 2.49 mg/kg in Control, Trial

1, and Trial 2, respectively, as shown in Fig. 7. The maximum increment of available phosphorus and total phosphorus was observed in Trial 2, when 5% MSW char was co-composted with vegetable waste, compared to Trial 1 and Control which was comparable to biochar addition with compost (Doan et al. 2015). Bacterial mineralization and the decomposition of organic biomass during the composting process lead to an increase in phosphorus (Kausar et al. 2020).

### Variation in C/N ratio during composting period

Another important parameter that is crucial for nutrient balance and microbial growth during the composting process is the C/N ratio. Microorganisms mostly obtain their resources from carbon, while nitrogen is crucial for the synthesis of the protozoa that make up cells. Analyzing the

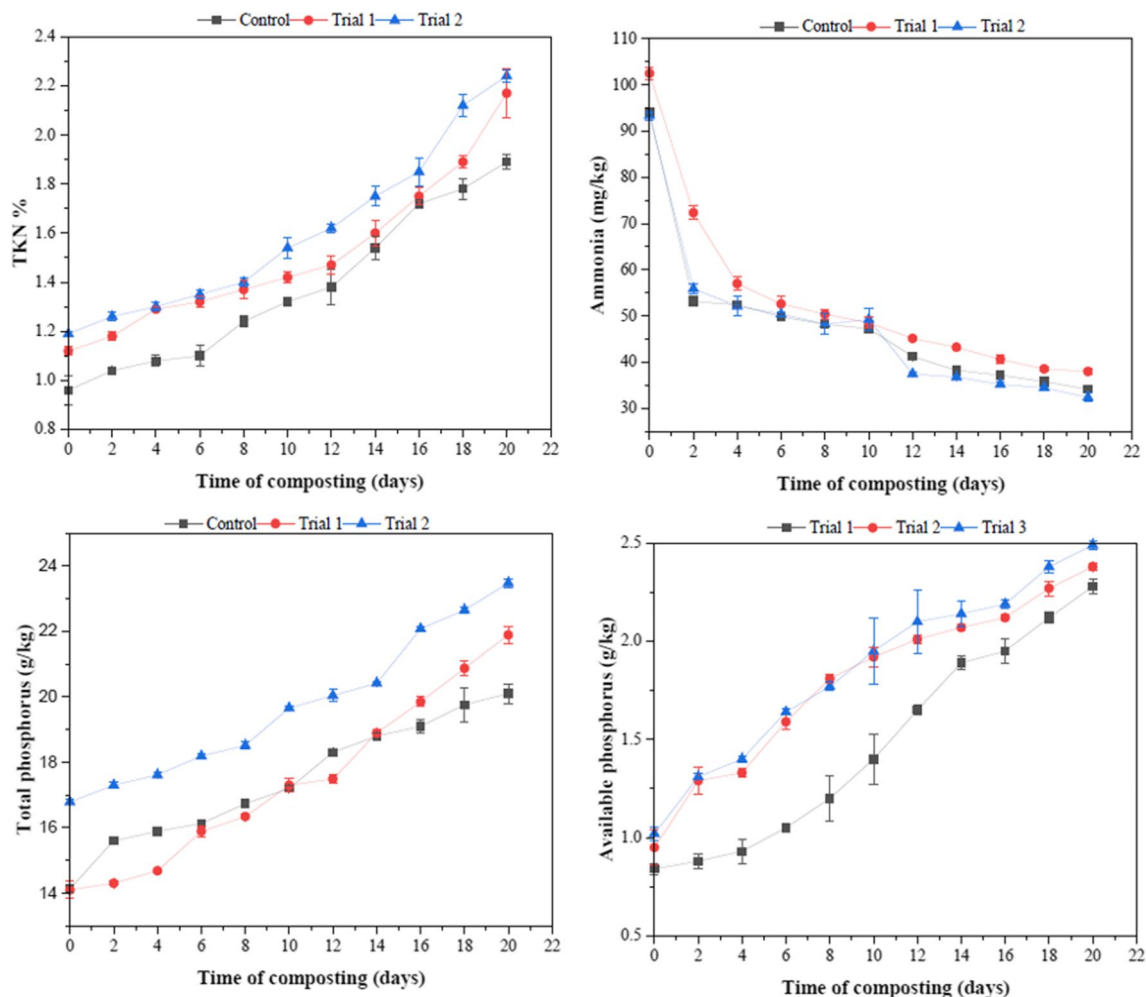


Fig. 7 Nitrogen dynamics (TKN and NH<sub>4</sub>-N) and phosphorus (TP and AP) dynamics during the composting period

alterations in the C/N ratio allows for the measurement of organic matter decomposition and the stabilization of compost. A C/N ratio exceeding 30/1 could lead to a reduction in the activity of microbes, and below 18/1 may result in nitrogen loss to the atmosphere as ammonia. Therefore, the C/N ratio between 19 and 30 is ideal for microbes during composting (Kauser et al. 2020). In the present study, C/N reduced from 28.55, 28.9, and 22.54 to 11.83, 12.09, and 10 in Control, Trial 1, and Trial 2, respectively, as shown in Fig. 8. Final compost with a C/N ratio between 10 and 15 indicates good degree of maturity (Sudharsan Varma and Kalamdhad 2015). It was observed that when 2.5% of MSW char was added during the co-composting of vegetable waste, the final product had much better maturity as compared to 5% MSW char and control. The range of the C/N ratio for a matured compost was within the range when MSW char was applied during composting akin to biochar (Guo et al. 2020).

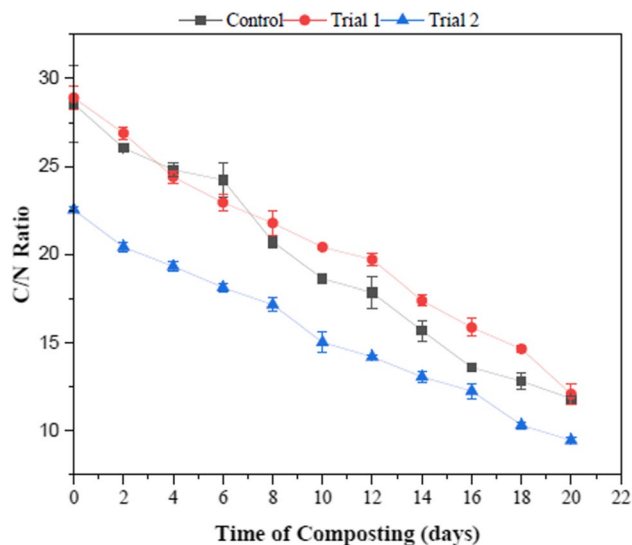


Fig. 8 Variation in C/N ratio during 1 composting

## Variation of macronutrients during the composting period

Potassium is the third most important macronutrient required by the plants for its growth whereas magnesium is required by the plants for chlorophyll production. Calcium is the secondary macronutrient required by the plant for the cell division. It was observed that with the addition of MSW char, the total potassium increased from 3.08, 3.01, and 3.12 to 5.86, 6.9, 6.13 g/kg in Control, Trial 1, and Trial 2, respectively, as shown in Fig. 9. The other macronutrients such as total Na, Mg, and Ca exhibited an upward trend during composting for all trials. The final values found to be 4.23 g/kg (Control), 4.73 g/kg (Trial 1), and 4.58 g/kg (Trial 2) of sodium; 40.89 g/kg (Control), 44.9 g/kg (Trial 1), and 51.79 g/kg (Trial 2) of calcium; and 3.14 g/kg (Control), 3.3 g/kg (Trial 1), and 3.32 g/kg (Trial 2) of magnesium. The highest concentration of macronutrients was observed

in Trial 2 when 5% of MSW char was added, which also indicated the highest reduction of volatile solids and was comparable with the co-composting of biochar (Jain et al. 2018a, b). The concentration of total Mg, Na, Ca, and K increased due to the loss of dry mass of materials caused by the decomposition of organic matter and subsequent mineralization during the composting process.

## sCOD, sBOD, and variation of CO<sub>2</sub> evolution rate during the composting period

Composting involves the aerobic decomposition of organic matter. Changes in sBOD and sCOD levels depend on the organic material degradation. The sBOD and sCOD decreased in all trials during the composting process due to vegetable waste degradation, as shown in Fig. 10. In Trial 2, there was a maximum reduction in

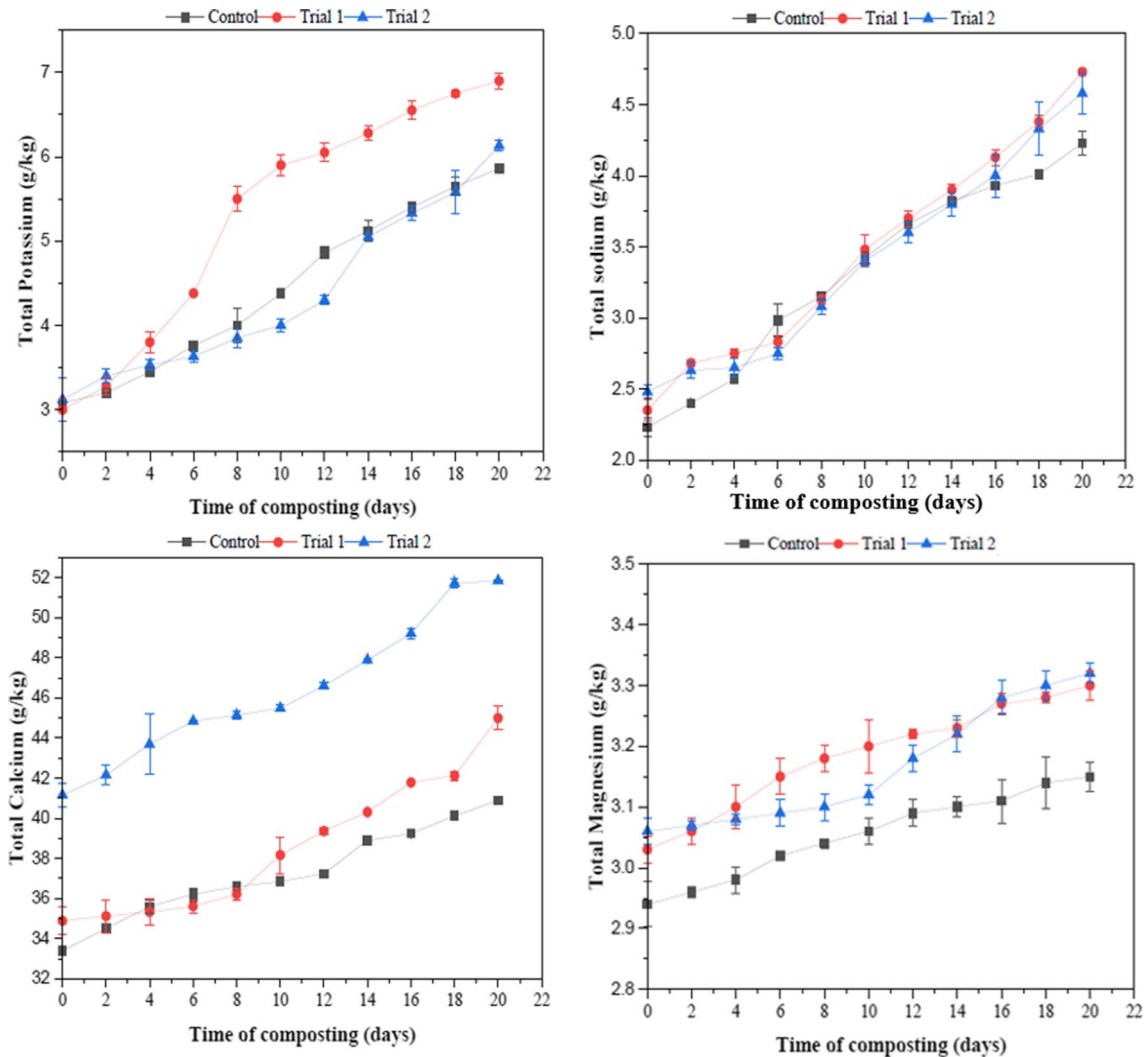


Fig. 9 Variation of macronutrients: potassium, sodium, calcium, and magnesium during the composting period

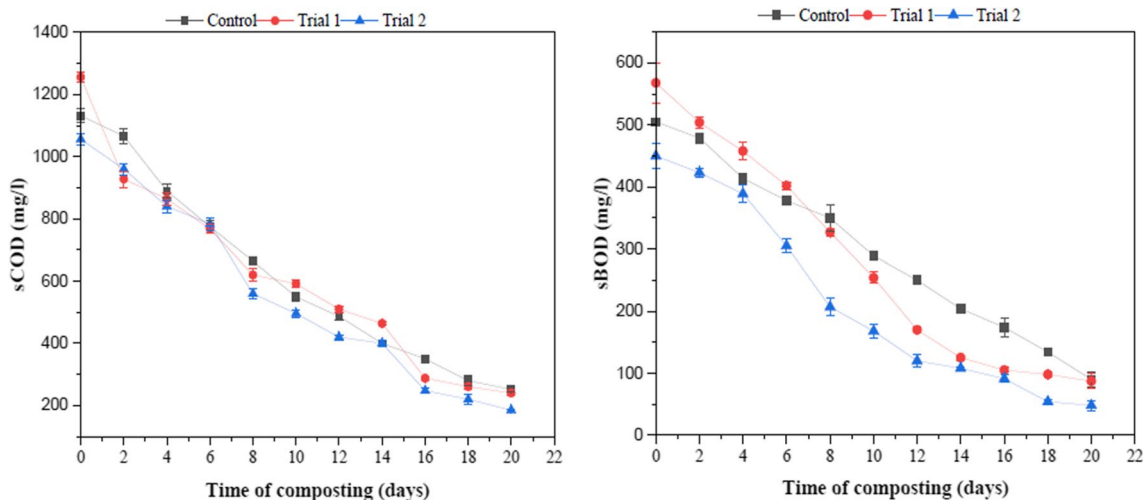


Fig. 10 sCOD and sBOD during composting period

sBOD (89.33%) followed by Trial 1 (84.68%) and Control (83%). There was no significant difference in the reduction of the body after 18 days of composting in Trial 1 and Trial 2. Initially, sCOD was in the range of 505, 568, and 450 mg/L and finally reduced to 90, 87, and 48 mg/L in Control, Trial 1, and Trial 2, respectively, during composting. The degradation of organic matter by microbes during the composting reduces sBOD and sCOD, which in turn lowers carbon dioxide emissions. The emission of CO<sub>2</sub> decreased because of a decrease in sBOD and sCOD, indicating that the compost had stabilized.

The most accurate method for assessing the stability of compost is CO<sub>2</sub> evolution as it detects carbon that comes directly from the compost under evaluation. Aerobic respiration has a direct relationship with CO<sub>2</sub> emission. As shown in Fig. 11, CO<sub>2</sub> emission decreases at the final stages of composting due to a decrease in degradable organic matter and lower microbial activity.

**Variation of heavy metals (Fe, Pb, Mn, Zn, Cr, Cu, and Ni) during the composting period**

Throughout composting, an increase in heavy metal concentration has been noted, attributed to material loss resulting from organic matter mineralization. Figure 12 illustrates the total concentration of heavy metal during rotary drum composting in Control, Trial 1, and Trial 2. According to Singh and Kalamdhad (2012), the increase in total heavy metal content is the result of mass degradation during composting due to organic matter breakdown, CO<sub>2</sub>, and moisture emission (Maturi et al., 2021).

**Microbial counts**

The hygiene of compost can be determined by the presence of coliform bacteria. The recommended values of fecal density for compost hygienization are  $5 \times 10^2$  and  $5 \times 10^3$  MPN/g dry weight (Sudharsan Varma and Kalamdhad 2015). The average number of total coliforms was observed in the range of  $2.1 \times 10^7$ ,  $1.7 \times 10^7$ , and  $3.3 \times 10^7$  MPN/g dry weight and finally reduced to  $3.3 \times 10^4$ ,  $2.4 \times 10^4$ , and  $2.4 \times 10^4$  MPN/g dry weight in Control, Trial 1, and Trial 2, respectively, as shown in Table 3. However, Fecal coliform was in the order of  $2.1 \times 10^6$ ,  $1.4 \times 10^6$ , and  $2.0 \times 10^6$  MPN/g dry weight reduced to  $2.0 \times 10^3$ ,  $2.1 \times 10^3$ , and  $1.1 \times 10^3$  MPN/g dry weight in Control, Trial 1, and Trial 2. Maximum reduction

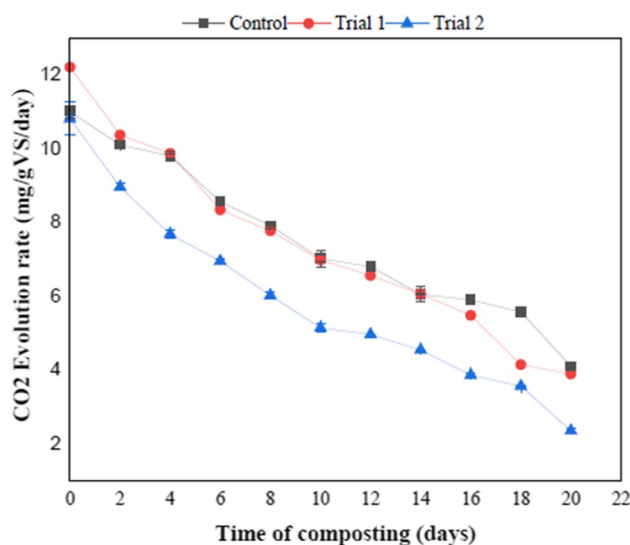
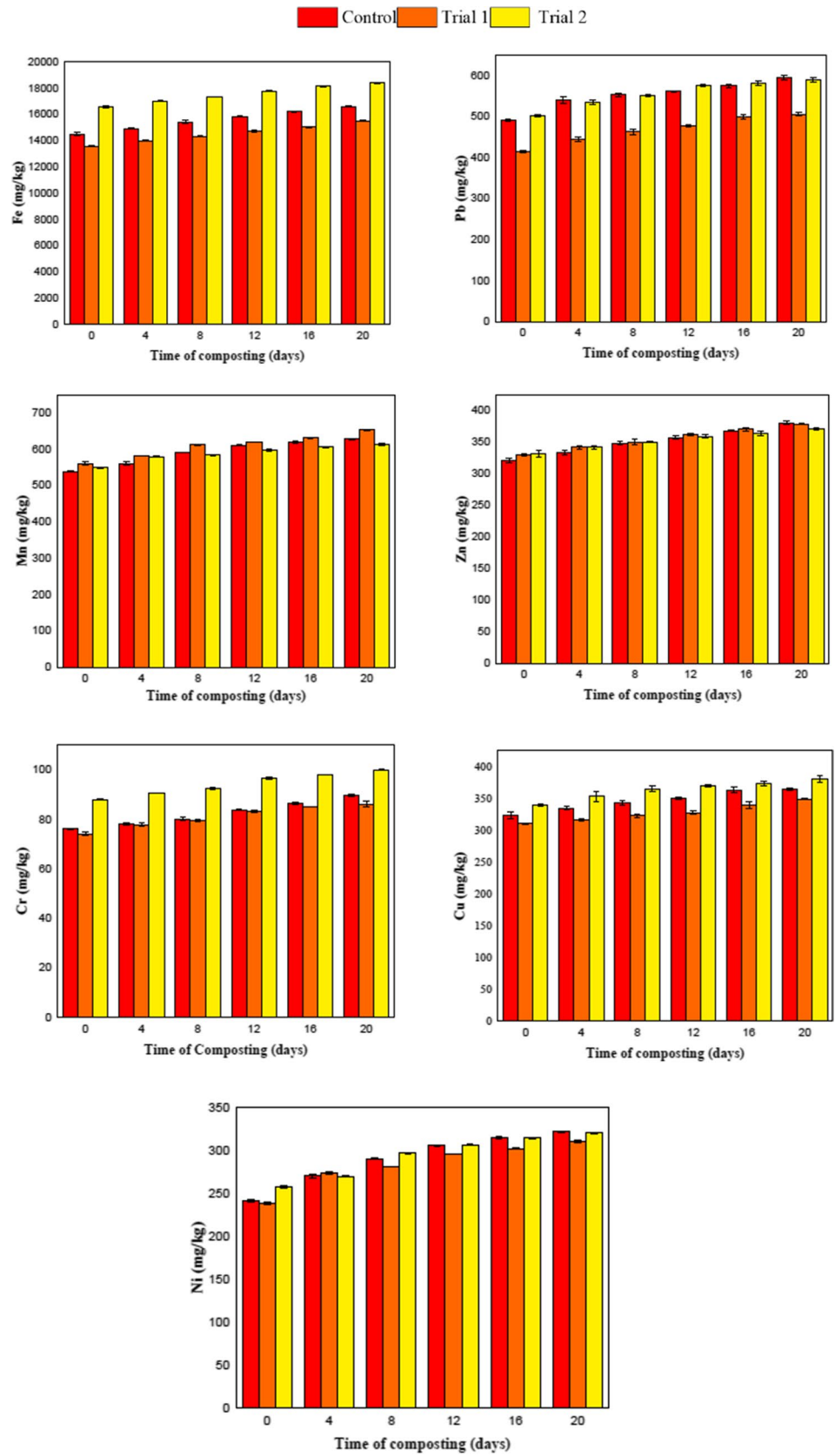


Fig. 11 Variation CO<sub>2</sub> evolution rate during the composting period

**Fig. 12** Variation of heavy metals (Fe, Pb, Mn, Zn, Cr, Cu, and Ni) during the composting period



**Table 3** Total and fecal coliform count during composting

Trials	Total coliform			Fecal coliform		
	0th day	10th day	20th day	0th day	10th day	20th day
Control	$2.1 \times 10^7$	$1.1 \times 10^5$	$3.3 \times 10^4$	$2.1 \times 10^6$	$2.1 \times 10^4$	$2.0 \times 10^4$
Trial 1	$1.7 \times 10^7$	$2.0 \times 10^5$	$2.4 \times 10^4$	$1.4 \times 10^6$	$1.7 \times 10^4$	$2.1 \times 10^3$
Trial 2	$3.3 \times 10^7$	$2.2 \times 10^5$	$2.4 \times 10^4$	$2.0 \times 10^6$	$1.0 \times 10^5$	$1.1 \times 10^3$

**Table 4** Total heterotrophic colonies during composting

Trials	Total Heterotrophs (CFU/g)	
	0 day	20 days
<b>Control</b>	$1.84 \times 10^{11}$	$2.1 \times 10^6$
<b>Trial 1</b>	$2.12 \times 10^{12}$	$1.23 \times 10^6$
<b>Trial 2</b>	$2.72 \times 10^{12}$	$1.04 \times 10^6$

of total coliform and fecal coliform was observed in Trial 2 due to high temperature (53.8 °C).

### Heterotrophic plate count

Due to the high amount of initial waste composition, the microbial population was very high during the initial phase of composting. The mesophilic heterophilic bacteria utilize the highly biodegradable organic matter for cell energy and cell division, thereby increasing the temperature of the composting environment. Therefore, there is a gradual decrease in heterotrophic bacteria after the thermophilic phase. The number of heterotrophs was detected as  $1.84 \times 10^{11}$ ,  $2.12 \times 10^{12}$ , and  $2.72 \times 10^{12}$  CFU/g dry weight and finally reduced to  $2.1 \times 10^6$ ,  $1.23 \times 10^6$ , and  $1.04 \times 10^6$  CFU/g dry weight in Control, Trial 1, and Trial 2, respectively, as shown in Table 4. Maximum reduction of total heterotrophic was observed in Trial 2 due to high temperature (53.8 °C).

### Conclusion

The findings of the study suggest that utilizing rotary drum composting for vegetable waste, in conjunction with MSW char, has proven to be a successful approach in terms of biodegradation, nutrients, and heavy metals adsorption. This process allows for the production of nutrient-rich compost in just 20 days. The introduction of MSW char into the mix enhances the aeration of the composting materials, which accelerates the decomposition process. During the initial composting stages, there was a noticeable increase in temperature, with Trial 2 reaching the highest temperature recorded at 53.8 °C. Trial 2 also

exhibits a prolonged thermophilic phase due to the higher quantity of MSW char, signifying greater organic matter degradation during this phase. Additionally, incorporating MSW char into the composting process raises the pH levels in all treatments compared to the control, indicating strong buffering capacity. Trial 2 demonstrates a more pronounced increase in electrical conductivity compared to the control and Trial 1; although it decreased in the later stages of composting. Furthermore, all trials exhibit improved nutritional properties when MSW char is added during composting, and there is a reduction in the concentration of heavy metals compared to the control. Therefore, the inclusion of MSW char not only enhances the quality and speed of composting but also encourages the transformation of mixed MSW into valuable products.

**Supplementary Information** The online version contains supplementary material available at <https://doi.org/10.1007/s11356-024-34332-4>.

**Acknowledgements** The authors are grateful to the Department of Civil Engineering, Central Instrumentation Facility, and School of Agro and Rural Technology at the Indian Institute of Technology Guwahati, India, for providing workspace and carrying out PXRD, FESEM, TGA/DTA, and FTIR analysis.

**Author contribution** Silvia Saikia: data curation, conceptualization, writing—original draft, methodology, software. Krishna Chaitanya Maturi: methodology, writing—review and editing. Harsh Prit: data curation, methodology, software. Suryateja Pottipati: methodology, writing—review and editing. Ajay S. Kalamdhad: supervision, conceptualization, writing—review and editing.

**Data Availability** All data, models, or experimental frameworks used during the study are available from the corresponding author by request.

### Declarations

**Ethics Approval** The authors declare that the submitted manuscript is original. They also acknowledge that the current research has been conducted ethically and that the final shape of the research has been agreed upon by all the authors.

**Consent to participate** The authors consent to participate in this research study.

**Consent for publication** The authors consent to publish the current research in “Environmental Science and Pollution Research” journal.

**Conflict of interest** The authors declare no competing interests.

## References

- Agyarko-Mintah E, Cowie A, Van Zwieten L, Singh BP, Smillie R, Harden S, Fornasier F (2017) Biochar lowers ammonia emission and improves nitrogen retention in poultry litter composting. *Waste Manag* 61:129–137. <https://doi.org/10.1016/j.wasman.2016.12.009>
- Antonangelo JA, Sun X, Zhang H (2021) The roles of co-composted biochar (COMBI) in improving soil quality, crop productivity, and toxic metal amelioration. *J Environ Manag* 277. <https://doi.org/10.1016/j.jenvman.2020.111443>
- Awasthi MK, Wang Q, Chen H, Wang M, Ren X, Zhao J, Li J, Guo D, Li D, Sheng, Awasthi, S. K., Sun, X., & Zhang, Z. (2017) Evaluation of biochar amended biosolids co-composting to improve the nutrient transformation and its correlation as a function for the production of nutrient-rich compost. *Biores Technol* 237:156–166. <https://doi.org/10.1016/j.biortech.2017.01.044>
- Brandi J, Wilson-Wilde L (2013) Standard methods. *Ency of Forensic Sci: 2nd Ed* 522–527. <https://doi.org/10.1016/B978-0-12-382165-2.00237-3>
- Busch D, Glaser B (2015) Stability of co-composted hydrochar and biochar under field conditions in a temperate soil. *Soil Use Manag* 31(2): 251–258. <https://doi.org/10.1111/sum.12180>
- Camps M, Tomlinson T (2015) The use of biochar in composting. International Biochar Initiative, 1–4
- Doan TT, Henry-Des-Tureaux T, Rumpel C, Janeau JL, Jouquet P (2015) Impact of compost, vermicompost and biochar on soil fertility, maize yield and soil erosion in Northern Vietnam: a three year mesocosm experiment. *Sci Total Environ* 514:147–154. <https://doi.org/10.1016/j.scitotenv.2015.02.005>
- Feng Y, Wang G, Zhen L, Y., Wang, Cheng, D., Miao, Fan, S., Hu, Zhao, Q., Sheng, Xue, J., Zhang, S., Qing, & Li, Z. Jun. (2021) The impacts of oxytetracycline on humification during manure composting can be alleviated by adjusting initial moisture contents as illustrated by NMR. *J Integr Agric* 20(8):2277–2288. [https://doi.org/10.1016/S2095-3119\(20\)63332-9](https://doi.org/10.1016/S2095-3119(20)63332-9)
- Gao S, Harrison BP, Thao T, Gonzales ML, An D, Ghezzehei TA, Diaz G, Ryals RA (2023) Biochar co-compost improves nitrogen retention and reduces carbon emissions in a winter wheat cropping system. *GCB Bioenergy* 15(4):462–477. <https://doi.org/10.1111/gcbb.13028>
- Godlewska P, Schmidt HP, Ok YS, Oleszczuk P (2017) Biochar for composting improvement and contaminants reduction. *A Review Bioresource Technology* 246(May):193–202. <https://doi.org/10.1016/j.biortech.2017.07.095>
- Guo X, xia, Liu, H. tao, & Zhang, J. (2020) The role of biochar in organic waste composting and soil improvement: a review. *Waste Manage* 102:884–899. <https://doi.org/10.1016/j.wasman.2019.12.003>
- Hazarika J, Khwairakpam M (2018) Evaluation of biodegradation feasibility through rotary drum composting recalcitrant primary paper mill sludge. *Waste Manage* 76:275–283. <https://doi.org/10.1016/j.wasman.2018.03.044>
- Jacoby R, Peukert M, Succurro A, Koprivova A, Kopriva S (2017) The role of soil microorganisms in plant mineral nutrition—current knowledge and future directions. *Front Plant Sci* 8(September):1–19. <https://doi.org/10.3389/fpls.2017.01617>
- Jain MS, Daga M, Kalamdhad AS (2018a) Composting physics: a science behind bio-degradation of lignocellulose aquatic waste amended with inoculum and bulking agent. *Process Saf Environ Prot* 116:424–432. <https://doi.org/10.1016/j.psep.2018.03.017>
- Jain MS, Jambhulkar R, Kalamdhad AS (2018b) Biochar amendment for batch composting of nitrogen rich organic waste: effect on degradation kinetics, composting physics and nutritional properties. *Biores Technol* 253(January):204–213. <https://doi.org/10.1016/j.biortech.2018.01.038>
- Kalamdhad AS, Pasha M, Kazmi AA (2008) Stability evaluation of compost by respiration techniques in a rotary drum composter. *Resour Conserv Recycl* 52(5):829–834. <https://doi.org/10.1016/j.resconrec.2007.12.003>
- Kausar H, Pal S, Haq I, Khwairakpam M (2020) Evaluation of rotary drum composting for the management of invasive weed *Mikania micrantha* Kunth and its toxicity assessment. *Biores Technol* 313(April):123678. <https://doi.org/10.1016/j.biortech.2020.123678>
- Lashari MS, Liu Y, Li L, Pan W, Fu J, Pan G, Zheng J, Zheng J, Zhang X, Yu X (2013) Effects of amendment of biochar-manure compost in conjunction with pyroigneous solution on soil quality and wheat yield of a salt-stressed cropland from Central China Great Plain. *Field Crop Res* 144:113–118. <https://doi.org/10.1016/j.fcr.2012.11.015>
- Mangkoedihardjo, S. (2006). Reevaluation of maturity and stability indices for compost. *Journal of Applied Sciences and Environmental Management*, 10(3). <https://doi.org/10.4314/jasem.v10i3.17324>
- Maturi KC, Haq I, Kalamdhad AS (2022a) Biodegradation of an intrusive weed *Parthenium hysterophorus* through in-vessel composting technique: toxicity assessment and spectroscopic study. *Environ Sci Pollut Res* 29(56):84600–84615. <https://doi.org/10.1007/s11356-022-21816-4>
- Maturi KC, Haq I, Kalamdhad AS (2022b) Performance assessment of in-vessel composter through heavy metal immobilization and humification of *Parthenium hysterophorus*. *Bioresour Technol* 360:127626. <https://doi.org/10.1016/j.biortech.2022.127626>
- Maturi KC, Kalamdhad AS (2024) Bioconversion of *Lantana camara* into an agricultural bioproduct through rotary drum composter. *Biomass Convers Biorefinery* 14:1389–1404. <https://doi.org/10.1007/s13399-023-05137-1>
- Maturi KC, Banerjee A, Kalamdhad AS (2021) Assessing mobility and chemical speciation of heavy metals during rotary drum composting of *Ageratum conyzoides*. *Environ Technol Innov* 24:101871. <https://doi.org/10.1016/j.eti.2021.101871>
- Meena, A. L., Karwal, M., & Dutta, D. (2021). *Composting: phases and factors responsible for efficient and improved composting network project on organic farming view project*. January. <https://doi.org/10.13140/RG.2.2.13546.95689>
- Munera-Echeverri JL, Martinsen V, Strand LT, Zivanovic V, Cornelissen G, Mulder J (2018) Cation exchange capacity of biochar: an urgent method modification. *Sci Total Environ* 642:190–197. <https://doi.org/10.1016/j.scitotenv.2018.06.017>
- Murtaza G, Usman M, Iqbal J, Hyder S, Solangi F, Iqbal R, Okla MK, Ahmed A, Ghamdi A, Elsalahy HH, Tariq W, Elwany OAAIAI (2024) Liming potential and characteristics of biochar produced from woody and non-woody biomass at different pyrolysis temperatures. *Sci Rep* 1–12. <https://doi.org/10.1038/s41598-024-61974-8>
- Oldfield TL, Sikirica N, Mondini C, López G, Kuikman PJ, Holden NM (2018) Biochar, compost and biochar-compost blend as options to recover nutrients and sequester carbon. *J Environ Manag* 218:465–476. <https://doi.org/10.1016/j.jenvman.2018.04.061>
- Qu Y, Qu J, Yan W, Yue T, Zhang Q, Yi W, Liu X, Sun Y (2022) Influence of biochar on physico-chemical, microbial community and maturity during biogas residue aerobic composting process. *Fermentation* 8(11). <https://doi.org/10.3390/fermentation8110623>
- Rodríguez-Vila A, Forján R, Guedes RS, Covelo EF (2016) Changes on the phytoavailability of nutrients in a mine soil reclaimed with compost and biochar. *Water Air Soil Pollut* 227(12). <https://doi.org/10.1007/s11270-016-3155-x>
- Saikia S, Kalamdhad AS (2023) Response surface methodology (RSM)-based pyrolysis process parameter optimization for char generation from municipal solid waste (MSW) in a fixed bed



- reactor. *Sustainable Energy Technol Assess* 60(July):103541. <https://doi.org/10.1016/j.seta.2023.103541>
- Sharma D, Varma VS, Yadav KD, Kalamdhad AS (2017) Evolution of chemical and biological characterization during agitated pile composting of flower waste. *Int J Recycl Org Waste Agric* 6(1):89–98. <https://doi.org/10.1007/s40093-017-0155-9>
- Singh J, Kalamdhad AS (2012) Concentration and speciation of heavy metals during water hyacinth composting. *Biores Technol* 124:169–179. <https://doi.org/10.1016/j.biortech.2012.08.043>
- Singh J, Kalamdhad AS (2016) Effect of lime on speciation of heavy metals during composting of water hyacinth. *Front Environ Sci Eng* 10(1):93–102. <https://doi.org/10.1007/s11783-014-0704-7>
- Sudharsan Varma V, Kalamdhad AS (2015) Evolution of chemical and biological characterization during thermophilic composting of vegetable waste using rotary drum composter. *Int J Environ Sci Technol* 12(6):2015–2024. <https://doi.org/10.1007/s13762-014-0582-3>
- Teodoro M, Trakal L, Gallagher BN, Šimek P, Soudek P, Pohořelý M, Beesley L, Jačka L, Kovář M, Seyedsadr S, Mohan D (2020) Application of co-composted biochar significantly improved plant-growth relevant physical/chemical properties of a metal contaminated soil. *Chemosphere* 242. <https://doi.org/10.1016/j.chemosphere.2019.125255>
- Varma VS, Dhamodharan K, Kalamdhad AS (2018) Characterization of bacterial community structure during in-vessel composting of agricultural waste by 16S rRNA sequencing. *3 Biotech* 8(7):1–8. <https://doi.org/10.1007/s13205-018-1319-7>
- Wang Y, Villamil MB, Davidson PC, Akdeniz N (2019) A quantitative understanding of the role of co-composted biochar in plant growth using meta-analysis. *Sci Total Environ* 685:741–752. <https://doi.org/10.1016/j.scitotenv.2019.06.244>
- Wong JWC, Fung SO, Selvam A (2009) Coal fly ash and lime addition enhances the rate and efficiency of decomposition of food waste during composting. *Biores Technol* 100(13):3324–3331. <https://doi.org/10.1016/j.biortech.2009.01.063>
- Ye S, Zeng G, Wu H, Liang J, Zhang C, Dai J, Xiong W, Song B, Wu S, Yu J (2019) The effects of activated biochar addition on remediation efficiency of co-composting with contaminated wetland soil. *Resour Conserv Recycl* 140:278–285. <https://doi.org/10.1016/j.resconrec.2018.10.004>

**Publisher's Note** Springer Nature remains neutral with regard to jurisdictional claims in published maps and institutional affiliations.

Springer Nature or its licensor (e.g. a society or other partner) holds exclusive rights to this article under a publishing agreement with the author(s) or other rightsholder(s); author self-archiving of the accepted manuscript version of this article is solely governed by the terms of such publishing agreement and applicable law.